Title

The QCD phase transition and supernova core collapse

Journal

The Astrophysical Journal, 414(2)

ISSN

0004-637X

Authors

Gentile, NA
Aufderheide, MB
Mathews, GJ
et al.

Publication Date

1993-09-01

DOI

10.1086/173116

Peer reviewed

THE ASTROPHYSICAL JOURNAL, 414:701–711, 1993 September 10

THE QCD PHASE TRANSITION AND SUPERNOVA CORE COLLAPSE

N. A. GENTILE, M. B. AUFDERHEIDE, AND G. J. MATHEWS
University of California, Lawrence Livermore National Laboratory, Livermore, CA 94550
F. D. SWESTY
Department of Physics and Department of Earth and Space Sciences,
State University of New York at Stony Brook, Stony Brook, NY 11794
AND
G. M. FULLER
University of California, San Diego, La Jolla, CA 92093-0319
Received 1993 January 21; accepted 1993 March 12

ABSTRACT

We examine the implications for stellar core collapse of a phase transition occurring at densities of a few times nuclear matter density. We use a schematic equation of state motivated by the Skyrme model low-energy approximation to QCD, which contains a phase transition corresponding to the conversion of bulk nuclear matter to a chirally symmetric quark-gluon phase. We analyze the stability of the core against gravitational collapse with respect to the amount of gravitational binding energy released and the kinematic energy of the shock. We show that a first-order phase transition actually gives rise to two shocks which quickly coalesce. More importantly, we show that there are significant differences in the evolution of cores with or without first- or second-order phase transitions which may eventually lead to observational signatures in the neutrino signal.

Subject headings: stars: interiors — stars: neutron — supernovae: general

1. INTRODUCTION

The process of core collapse in supernovae converts gravitational potential energy of the collapsing core into internal and kinetic energy of an outward propagating shock wave (Colgate & White 1966; Bruenn, Arnett, & Schramm 1977; Wilson 1985; Bethe & Wilson 1985; Bruenn 1989a, b; Myra & Bludman 1989; Cooperstein & Baron 1990). The mechanism of this conversion is complicated. A complete analysis of shock formation requires, among other things, detailed modeling of neutrino transport (Mazurek 1975; Schramm & Arnett 1975; Bowers & Wilson 1982; Mayle 1990), general relativity (Van Riper 1979; Baron 1985; Baron, Cooperstein, & Kahana 1985a), and convection (Livio, Buchler, & Colgate 1980; Smarr et al. 1981; Wilson & Mayle 1988; Herant, Benz, & Colgate 1992; Burrows & Fryxell 1992; Miller, Wilson, & Mayle 1992). During the initial stages of collapse and bounce, the equation of state (EOS) describing densities greater than nuclear matter is also an important input into a simulation. It determines the dynamics of the collapse and the energy of the initial core bounce (van Riper & Arnett 1978; Bethe et al. 1979; Cooperstein & Baron 1990).

The evolution of the equation of state during supernova core collapse is the focus of the present study; in particular we examine the effects of a phase transition from nuclear matter to quark matter. An important parameter describing equations of state is Γ_1, the adiabatic index, defined by

$$\Gamma_1 = \frac{n}{P}\left(\frac{\partial P}{\partial n}\right)_s , \quad (1)$$

where n is the baryon number density and P is the pressure. A larger, i.e., stiffer, adiabatic index can cause the collapse to halt more rapidly and at a lower central density, leaving behind a less compact core, and providing less gravitational potential energy to the shock.

Phase transitions are important in modeling the collapse because of their effect on the behavior of the pressure and the adiabatic index as matter is compressed. Phase coexistence is possible when two phases have equal pressures and chemical potentials at the same temperature. In supernovae, dynamical time scales are on the order of milliseconds, while nucleon-nucleon reactions proceed on strong interaction time scales, around 10^{-21} seconds. Thus, the different phases of baryonic matter during a collapse will be in thermal equilibrium (Lattimer & Swesty 1991). Once neutrino trapping has occurred, the collapse will proceed adiabatically. If matter is adiabatically compressed through a first-order phase transition, the adiabatic index becomes very small (but not quite zero) as the less dense phase converts to the more dense phase. Since the compression is adiabatic rather than isothermal, the temperature of the two phases will increase. The pressure of the two phases will increase slightly, preventing the adiabatic index from becoming exactly zero (Pethick, Ravenhall, & Lattimer 1984). The behavior of pressure during a phase transition at constant entropy is illustrated schematically in Figure 1*a*. Figure 1*b* illustrates the behavior of the adiabatic index.

Takahara & Sato (1985, 1986) have investigated the effects of phase transitions on supernova explosions, using an idealized equation of state which contains a schematic phase transition above nuclear densities. In this paper, we investigate the effects of a more realistic phase transition in a more detailed fashion with high-resolution general relativistic numerical simulations.

In Newtonian theory it is possible to find a stable hydrostatic configuration for a spherical mass distribution if the adiabatic index exceeds 4/3 (cf. Chandrasekhar 1969, p. 583). Collapse ensues when the degeneracy pressure from relativistic

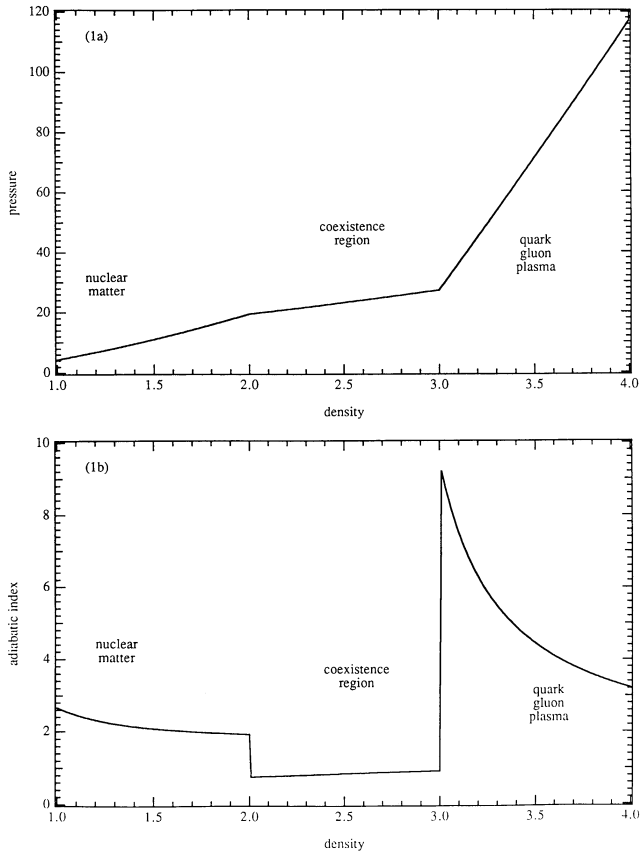

FIG. 1.—Pressure and adiabatic index vs. density for a schematic phase transition. (*a*) Pressure vs. density. (*b*) Adiabatic index vs. density.

electrons provides most of the pressure support for the star, since the equation of state for highly relativistic electrons has an adiabatic index of 4/3. At densities on the order of a tenth of nuclear matter density, the pressure of the nuclear phase is negative and increases with density, which lowers the value of Γ_1 below 4/3. The pressure becomes zero at nuclear matter density (Bethe et al. 1983; Lattimer & Swesty 1991). At densities greater than nuclear matter density, the equation of state stiffens. All equations of state developed to model matter at densities greater than nuclear density have adiabatic indices significantly greater than 4/3. A Newtonian body with a nuclear EOS will stop collapsing as the EOS stiffens, thereby producing a stable core. A phase transition which lowers Γ_1 just above nuclear density can make the collapse deeper and facilitate the release of more gravitational energy.

General relativity complicates this picture (Van Riper 1979; Baron 1985; Baron et al. 1985*a*). Stability of hydrostatic configurations requires that the pressure-averaged Γ_1 exceed 4/3 plus a term of order the ratio of the Schwarzschild radius to the stellar radius (Harrison et al. 1965). The conditions for stability then depend upon the structure and velocity, which become important in determining the outcome of collapse. If a sufficiently dense configuration is formed, the collapse may not stop even for $\Gamma_1 > 4/3$. Because a phase transition decreases pressure support, greater densities may be reached in a collapse. This may allow more gravitational energy to be released, or it may prevent the collapse from halting.

In this paper we examine the effects of a phase transition from nuclear matter to quark matter on spherical collapse with a fully general relativistic numerical hydrodynamics code. By using several different equations of state we vary the density and radius at which the phase transition occurs. These equations of state are motivated by field theoretic analyses of dense matter and its phase structure. We are interested in the effects of phase transitions on the dynamics at bounce, just as the proto-neutron star begins to form. The behavior of the density of the core during collapse and bounce is analyzed. The effect of different phase transitions on the amount of energy imparted to the shock is calculated by computing the kinetic energy and velocity of the shock, and the gravitational and internal energy released.

A study of shock stalling and the later development of the proto-neutron star at the core would require detailed modeling of the neutrino transport, which is beyond the scope of the present work. Neglecting neutrino transport at bounce is justified because only a small fraction, approximately 10^{51} ergs out of 10^{53} of the energy in neutrinos leaves the core within 10 milliseconds of bounce (Bruenn 1989a, b; Cooperstein & Baron 1990). The purpose of the present study is to identify the interesting regions of parameter space for subsequent studies of the later development of the core and of the resulting neutrino signal.

2. THE MODEL

Numerical simulation of collapse is accomplished with a fully general relativistic 1 + 1 dimensional computer program based on a finite difference formulation of the spherical general relativistic hydrodynamic equations (May & White 1967; van Riper 1979). Shocks are modeled using the artificial viscosity method. The equations of state used are discussed in the next sections.

After the initial collapse, the inner core settles into a quasi-static state close to hydrostatic equilibrium. The density and extent of this core will determine how much gravitational energy has been given to the shock in the collapse. We decompose the total mass-energy of the equilibrium core into a rest mass energy, a gravitational potential energy, and an internal energy (e.g., Weinberg 1972). Thus, one can determine how much energy the collapse makes available to the shock. In the following equations, natural units have been used: $G = c = \hbar = 1$.

If the material in the star were dispersed to infinity, it would have a total energy $m_b N$, where N is the number of baryons and m_b is the baryon rest mass. The observed mass-energy, m, at Schwarzschild radial coordinate r is given by

$$m(r) = \int_0^r 4\pi r'^2 \rho(r') dr' , \qquad (2)$$

where ρ is the total energy density. $M = m(R)$, where R is the radius of the star, is constant for a spherical collapse, because there are no spherical gravitational radiation modes to remove energy (Birkhoff's theorem).

The difference between the total energy and the energy at infinity is the binding energy,

$$E = M - m_b N . \qquad (3)$$

This is a measure of how much energy is released by the formation of a star from a diffuse assembly of baryons. Because M and N are constant, E is also. The total baryon number of the star, N, can be expressed in terms of $n(r)$, the number density of

baryons in a local inertial frame

$$N = \int_0^R 4\pi r^2 n(r)\left[1 - \frac{2m(r)}{r}\right]^{-1/2} dr \,. \quad (4)$$

The total energy density can be decomposed into contributions from rest mass and internal energy per volume $e(r)$

$$\rho(r) = m_b\, n(r) + e(r) \,. \quad (5)$$

Using equations (2) and (3) we may express $E = T + V$, where

$$T = \int_0^R 4\pi r^2 e(r)\left[1 - \frac{2m(r)}{r}\right]^{-1/2} dr \,, \quad (6)$$

is the internal energy and

$$V = \int_0^R 4\pi r^2 \rho(r)\left\{1 - \left[1 - \frac{2m(r)}{r}\right]^{-1/2}\right\} dr \,, \quad (7)$$

is the gravitational potential energy of a spherical configuration. Note that this quantity is negative; to first-order in GM/r, it is the Newtonian expression for gravitational potential energy

$$V = -\int_0^R 4\pi r^2 \frac{M(r)}{r}\, dr \,. \quad (8)$$

Because E is constant, the decrease in V as the core collapses causes T to increase. This analysis only holds for static spherical configurations. We will therefore apply it only to the dense cores of our simulations, which are static after the shock has propagated outward.

For our purposes, the energy released will be determined from differences in V and T for final cores left behind by collapses which occur with and without a phase transition. A phase transition which results in a denser core makes more gravitational binding energy available to the shock, either through prompt hydrodynamic processes or through delayed neutrino heating.

3. SKYRMION EQUATION OF STATE FOR HIGH BARYON DENSITY

Asymptotic freedom guarantees the existence of a high-density phase of matter in which the relevant degrees of freedom are free quarks and gluons (Witten 1984). It is, however, difficult to accurately model the transition to this state. This is because the problem involves physics in the strong coupling nonperturbative regime of QCD. The existence of a first-order phase transition between this phase and nuclear matter depends, of course, on how the two phases are modeled, and many different results have been reported (Baym & Chin 1976; Farhi & Jaffe 1984; Bethe, Brown, & Cooperstein 1987).

Perturbative QCD gives an expression for the thermodynamic potential Ω in powers of α_s, the strong coupling constant (McLerran 1986). Perturbation theory is thus applicable when the strong coupling constant is small. The strong coupling constant is density and temperature dependent; it becomes small when either the quark chemical potential ($=\frac{1}{3}$ the baryon chemical potential), or the temperature, is large compared to the QCD energy scale, $\Lambda_{\rm QCD} = 200$ MeV. This corresponds to temperatures much greater than 200 MeV or number densities much greater than of $\Lambda_{\rm QCD}^3/(\hbar c)^3 \approx 1$ fm^{-3}, approximately 7 times nuclear matter density. In this perturbative regime, baryonic matter becomes an almost ideal gas of quarks and gluons (Collins & Perry 1975; Freedman & McLerran 1977a, b, c). In supernovae, the quark chemical potential will be of the order of $\frac{1}{3}$ the baryon mass (≈ 310 MeV) and the temperatures in a supernova will be on the order of 10 MeV (Wilson & Mayle 1988). Thus, the conditions during core collapse require some sort of extrapolation into the nonperturbative regime.

From the thermodynamic potential, one can form expressions for pressure, chemical potential, etc., and so obtain an equation of state (Landau & Lifshitz 1980). The perturbative QCD series expression for Ω does not converge, however, in the region of chemical potential and temperature of interest to supernova collapse.

Employing quantities from hadron physics such as particle masses to describe the high-density phase is inappropriate, inasmuch as these quantities are the result of the non-Coulombic behavior of the color field in the confining phase of the QCD vacuum. The observed masses of hadrons, and inferred quantities such as the string tension and the bag size, result from field configurations which are not dominant in the unconfined phase, where the vacuum does not exclude field lines and where the color field can spread (Polyakov 1978; Susskind 1979). Thus, the predictive power of these heuristic models is limited.

Lattice gauge simulations have been employed to study possible finite temperature phase transitions near zero baryon chemical potential in QCD. It is presently believed that a first-order transition at high temperature and zero baryon chemical potential may be unlikely (Brown et al. 1990). These calculations in the high temperature/low density limit do not necessarily represent the behavior of matter in the relatively low-temperature, high-density regime of supernova cores.

Effective field theories have been the basis for much recent work on high-density phase transitions because of their ability to provide nonperturbative descriptions of strong interaction phenomena (Walhout 1988, 1990; Wambach 1990). The Skyrme model, which represents baryons as solitons in a classical meson field theory, is motivated by the $1/N_c$ expansion of QCD (Witten 1983). The Skyrme model employs an effective Lagrangean based on a nonlinear sigma model. Numerical simulations of these Skyrmions allow the development of an equation of state for dense matter (Walhout 1988).

Three different phases can be modeled with this approach (Walhout 1990). At low density (<0.1 fm^{-3}), the theory describes a liquid phase which is a mixture of solid nuclear matter, and a Fermi gas of nucleons. At ~ 0.1 fm^{-3}, the solid phase becomes more energetically favorable. This second phase is a face centered cubic crystal of solitons. This phase represents infinite nuclear matter. Both these phases resemble those described by Friedman & Pandharipande (1981); the liquid phase has $\Gamma_1 = 2$, while the solid phase is much stiffer at low densities, with Γ_1 asymptoting to 2 as the density increases.

At higher densities a first-order transition occurs in the Skyrme model. Several factors suggest that this third phase describes quark matter. For one, the expectation value of σ, which measures chiral symmetry, changes from its vacuum value of unity in the low-density phase, to zero. Thus, chiral symmetry is restored in the high-density phase. For another, the distribution of baryon number in this phase is delocalized.

In the low-density phase, it is concentrated in the center of the cells used in the numerical calculations; in the high-density phase, it spreads out to the corners of the cell. Also, the pressure of the high-density phase asymptotically varies as $\rho^{1/3}$, and the kinetic energy density as $n^{4/3}$, both characteristics of a Fermi gas description of deconfined quark matter. In fact, the energy density of the high-density phase is well fit by a simple QCD bag model expression

$$\rho = \frac{9}{4}\left(\frac{3\pi^2}{N_f}\right)^{1/3}\left[1 + \frac{2\alpha_s}{3\pi}\right]n^{4/3} + B\,, \tag{9}$$

with $B = 66$ MeV fm^{-3} and $\alpha_s = 1.1$, and N_f is the number of quark flavors, which is two in a Skyrmion calculation with SU(2) symmetry. These values are in reasonable accord with the MIT bag model values and with fits based on hadronic spectra (Walhout 1988). The sound speed in the quark-gluon phase asymptotes to $1/3^{1/2}$ (the extreme relativistic Fermi gas value), rather than to unity, as the Friedman-Pandharipande EOS does. Therefore, the Skyrmion quark-gluon EOS is always causal. Walhout (1990) gives numerical fits to the free energy calculated from the Skyrmion simulations, and describes the resulting equation of state.

4. PHENOMENOLOGICAL EQUATIONS OF STATE

The model described above is based on a Lagrangean with chiral SU(2) symmetry, corresponding to only two quark flavors. Further, its use of the Skyrme Lagrangean instead of a more detailed representation of the full QCD Lagrangean is another approximation (Wambach 1990). The prediction of a first-order phase transition at a few times nuclear matter density is important, but the details of the phase transition given by the approximate treatment of the model may not be accurate. We therefore utilize a phenomenological EOS which keeps the essential features of the Skyrmion EOS but which allows us to vary some of the details of the phase transition. We will employ a parameterization of the quark-gluon phase that reproduces equation (9), but treat B and α_s as parameters, rather than use the values which result from the Skyrmion calculation. By parameterizing the equation of state in this way, we can explore the effect of varying the density at which the phase transition takes place.

The thermodynamic potential for the quark-gluon plasma, to first order in the strong coupling constant in the limit of massless quarks, is

$$\begin{aligned}\Omega = &-\frac{N_c N_f}{6}\left(\frac{7\pi^2 T^4}{30} + \mu^2 T^2 + \frac{\mu^4}{2\pi^2}\right) \\ &+ \frac{(N_c^2 - 1)N_f \alpha_s}{8\pi}\left(\frac{5\pi^2 T^4}{18} + \mu^2 T^2 + \frac{\mu^4}{2\pi^2}\right) \\ &- \frac{\pi^2}{45}(N_c^2 - 1)T^4 + \frac{\pi}{36}N_c(N_c^2 - 1)\alpha_s T^4\end{aligned} \tag{10}$$

(McLerran 1986). As noted above, the baryon chemical potential will be of the order of the baryon mass and temperatures will be on the order of 10 MeV, so we may assume that the temperature is small compared to the baryon chemical potential. We use $N_c = 3$, $N_f = 3$.

The above expression is applicable only in the perturbative regime of small α_s, i.e., large densities and temperatures. In this limit, baryonic matter is a relativistic Fermi gas with an equation of state $P = 1/3\rho$, where ρ is the energy density. The pressure calculated from this EOS is greater than that of nuclear matter at all densities, even at densities below that of nuclear matter. That is, the pure Fermi gas EOS is always the high-pressure phase. It does not exhibit a phase transition to a higher pressure, confined phase at low density. At low densities, nonperturbative effects lower the pressure of the quark-gluon phase, as lattice gauge calculations have shown (Brown et al. 1988). The transition to a hadronic phase at low density and pressure is modeled by adding a term, the bag constant B, to the thermodynamic potential: $\Omega_{\rm QCD} \rightarrow \Omega_{\rm QCD} + BV$, where V is the volume. Adding this phenomenological term lowers the pressure of the quark phase so that a transition to a confined phase occurs (Callen, Dashen, & Gross 1979; Berg et al. 1986).

Expressions for pressure, energy density, and chemical potential are obtained by the usual thermodynamic manipulations (Alcock, Fuller, & Mathews 1987; Fuller, Mathews, & Alcock 1988). To first order in the QCD coupling constant they are

$$\rho = \frac{9}{4}\left(\frac{3\pi^2}{N_f}\right)^{1/3}\left[1 + \frac{2\alpha_s}{3\pi}\right]n^{4/3} + B\,, \tag{11}$$

$$P = \frac{3}{4}\left(\frac{3\pi^2}{N_f}\right)^{1/3}\left[1 + \frac{2\alpha_s}{3\pi}\right]n^{4/3} - B\,, \tag{12}$$

and

$$\mu = 3\left(\frac{3\pi^2}{N_f}\right)^{1/3}\left[1 + \frac{2\alpha_s}{3\pi}\right]n^{1/3}\,. \tag{13}$$

Equations (11), (12), and (13) yield a simple EOS,

$$\rho = 3P + 4B\,. \tag{14}$$

The sound speed for the quark phase

$$c_s^2 = \left(\frac{\partial P}{\partial \rho}\right)_S = \frac{1}{3}\frac{P}{P + B} \tag{15}$$

asymptotes to the extreme relativistic Fermi gas limit from below, and is never acausal.

The adiabatic index,

$$\Gamma_1 = \frac{n}{P}\left(\frac{\partial P}{\partial n}\right)_S = \frac{4}{3}\frac{P + B}{P}\,, \tag{16}$$

asymptotes to the extreme relativistic limit, 4/3, from above.

The Skyrmion EOS does not saturate at nuclear density. We therefore use a schematic nuclear equation of state (Baron, Cooperstein, & Kahana 1985b) that approximately describes the pressure behavior of matter at and around nuclear density (i.e., $P = 0$ at nuclear density)

$$P = \frac{K n_{\rm nuclear}}{9\gamma}\left[u^\gamma - 1\right] \tag{17}$$

$$e = \frac{K}{9\gamma}\left[\frac{u^{\gamma-1} - \gamma}{\gamma - 1} + \frac{1}{u}\right] + e_s + e_b \tag{18}$$

$$\mu = \frac{\rho + P}{n}\,. \tag{19}$$

Here the saturation density $n_{\rm nuclear} = 0.155$ fm^{-3}, $u = n/n_{\rm nuclear}$, the compression modulus $K = 220$ MeV, $\gamma = 2.5$, the binding energy $e_b = -16$ MeV baryon^{-1}, and the symmetry energy $e_s = 31.5$ MeV baryon^{-1}. In equation (19), μ is the baryon chemical potential, ρ is the total energy density per baryon including rest mass, P is the pressure, and n is the baryon number density. This EOS is used from nuclear density ($u = 1$) until the phase transition. Above nuclear density, the dominant pressure contribution is from electrons. The pressure contribution of electrons and photons is calculated from the EOS given in Appendix C of Lattimer & Swesty (1991). This is an excellent approximation at high densities ($> 10^9$ g cm^{-3}). At lower densities, explicit solution of the appropriate Fermi integrals is necessary in order to calculate the thermodynamic properties of the electron gas (Cooperstein 1985).

A phase transition occurs between the phase represented by equations (17) through (19) and the phase represented by equations (11) through (13) when the chemical potentials and pressures of the two phases are equal. Table 1 lists some characteristics of the phase transitions exhibited by the equations of state used in the core collapses we modeled.

Figure 2 shows the pressure and total adiabatic index versus density for the phase transitions beginning at 1.5 $n_{\rm nuclear}$ in Table 1. As the phase transition density is increased, the adiabatic index of the quark phase at the transition density decreases. The greater the transition density, the less stiff the quark phase EOS. In all hydrodynamic calculations, however, collapse reached a maximum density only slightly greater than the quark phase density. Note that the adiabatic index assumes small but nonzero values while the density is in the range where the phases are in equilibrium. This is because the electron pressure is given by an equation of state that is independent of the state of baryonic matter. A more sophisticated model of the phase transition would couple the electrons to the baryonic matter.

From equation (13), we see that for a fixed equilibrium chemical potential, the density of the quark phase will be greater for smaller α_s. Thus, for a given μ, $\alpha_s = 0$ will give the phase transition with the greatest quark phase baryon number density. To explore the density range over which coexistence is possible, we set $\alpha_s = 0$, and vary B. This varies the width of the coexistence region pictured in Figure 1. If the chemical potential of the hadronic phase increases faster than $n^{1/3}$, a series of phase transitions at greater and greater density will be possible, because the quark matter chemical potential varies as $n^{1/3}$. Conversely, if the chemical potential of the hadronic phase increases less rapidly than $n^{1/3}$, the quark phase baryon number density increases more slowly than the hadron phase baryon number density, and the series of possible phase transitions will end with a second-order phase transition when

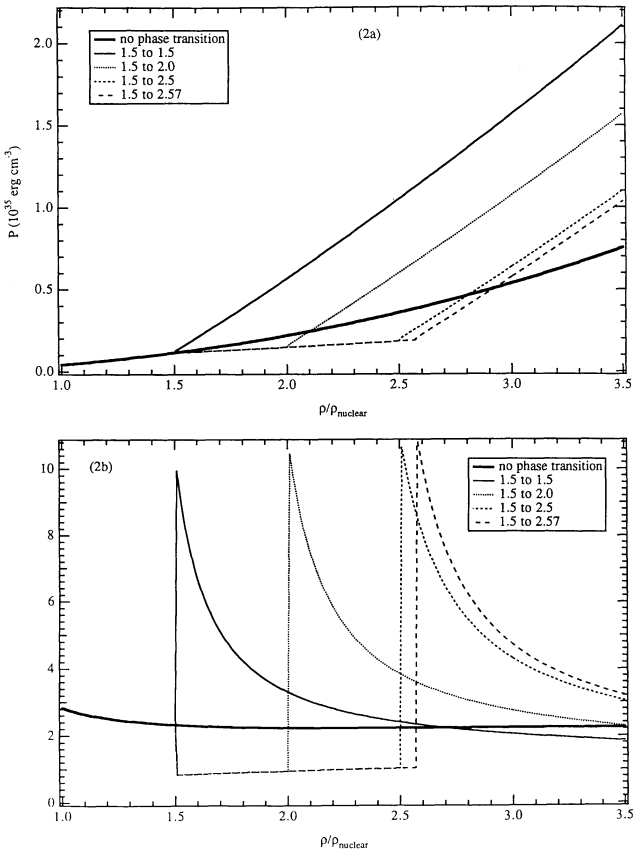

FIG. 2.—Pressure P and adiabatic index Γ vs. density ρ of phase transitions from hadronic phase to quark phase as a function of density ρ in units of $\rho_{\rm nuclear}$. Phase transitions begin at 1.5 $\rho_{\rm nuclear}$. (*a*) Pressure vs. density. (*b*) Adiabatic index vs. density.

TABLE 1

HADRON PHASE/QUARK PHASE EQUILIBRIUM

$n_{\rm hadron}$	$e_{\rm hadron}$	P_e	μ	$n_{\rm quark}$	$\rho_{\rm quark}$	$e_{\rm quark}$	B	α_s	$\Gamma_{1,\rm quark}$	$\Gamma_{1,\rm total}$
1.5.....	−8.41	0.426	940.9	1.5	3.88	−8.45	51.7	0.930	27.3	9.95
				2.0	5.18	−5.69	69.8	0.413	36.5	10.5
				2.5	6.47	−4.04	88.0	0.0462	45.4	10.6
				2.57	6.66	−3.85	90.7	0.0	46.8	10.1
2.0.....	−3.79	1.13	957.0	2.0	5.18	−3.79	66.7	0.502	13.9	7.41
				2.5	6.47	0.601	85.1	0.128	17.4	8.01
				2.71	7.01	1.96	92.9	0.0	18.9	8.40
2.5.....	2.33	2.16	975.4	2.5	6.47	2.33	80.5	0.221	9.31	5.91
				2.87	7.43	6.65	94.4	0.0	10.7	6.41

NOTES.—$n_{\rm hadron,quark}$ are the baryon number densities of the nuclear matter and quark phases, respectively, in units of $n_{\rm nuclear}$. $\rho_{\rm quark}$ is the rest mass density of the quark phase, in units of 10^{14} g cm^{-3}. $e_{\rm hadron,quark}$ are the internal energy densities of the nuclear matter and quark phases, respectively, in units of 10^{18} ergs g^{-1}. P_e is the equilibrium pressure of the phases, in units of 10^{34} ergs cm^{-3}. The baryon chemical potential, μ, is given in units of MeV. The bag constant, B, is given in units of MeV fm^{-3}. Given the baryon number density of the hadronic phase, the pressure and chemical potential of the phase transition are fixed by the nuclear matter EOS. Choosing the baryon number density of the quark phase then determines the values of the strong coupling constant and the bag constant. The adiabatic index of pure quark matter at the transition density, and the adiabatic index of the matter including the effects of lepton pressure, are listed.

$n_{quark} = n_{hadron}$, $\alpha_s = 0$. This situation holds for our particular choice of a nuclear equation of state. This can be seen in Table 1. Coexistence is possible between phases with $n_{hadron} = 1.5$ and $n_{quark} = 2.57$, but, for a phase transition beginning at $n_{hadron} = 2.5$, the widest possible phase transition for our choice of nuclear EOS extends only to $n_{quark} = 2.87$.

In our model we pick the density of the hadronic phase and the quark phase at equilibrium at $T = 0$. This fixes the two parameters B and α_s. We require $\alpha_s \geq 0$. Table 1 shows the phase transitions considered. For a given hadronic phase density, the set of possible phase transitions begins with a second-order phase transition, with the quark phase baryon number density equal to that of the hadronic phase. As the equilibrium quark phase density is increased, the value of the strong coupling constant falls, and the value of the bag constant increases. The set of possible phase transitions ends when the value of α_s reaches zero. As the density of the hadron phase at equilibrium increases, α_s decreases and B increases for a given quark phase equilibrium density.

The adiabatic index, Γ_1, of the quark phase, equation (16), is also given in Table 1. These values are very large but do not represent the actual adiabatic index of the material because a significant amount of pressure is provided by leptons. The actual adiabatic index includes pressure of electrons. The equation of state is still significantly stiffer after the phase transition. The actual Γ_1 of the matter is given in Table 1 also.

5. RESULTS

We began at $t = 0$ with a 13 $M_\odot$ progenitor with a 1.18 $M_\odot$ iron core (Nomoto & Hashimoto 1988). The inner 1.4 $M_\odot$ was evolved with a 1 + 1 dimensional general relativistic hydrodynamics program with full radiation transport. Electron capture had reduced the electron fraction in the center of the core to 0.3. Collapse to this point took 101.245 milliseconds, and the central density was 3.434×10^{13} g cm^{-3} (=0.133 times nuclear density). We then rezoned the core to provide the greater resolution necessary to observe the effects of the phase transition in the center. The first 50 zones, with a mass of 1.2 $M_\odot$, were divided into 250 zones; i.e., each zone was split into five equal mass zones. Subsequent evolution of this core is done with a general relativistic code without radiation transport.

From this initial condition, we ran hydrodynamic simulations, using the equations of state listed in Table 1, for a time of 3 milliseconds. The bounce occurred about 0.75 ms after the start of the simulation. We calculated the amount of gravitational potential energy and internal energy released by the collapse by integrating $T(r)$ and $V(r)$ (eqs. [6] and [7]) over the innermost 0.5 $M_\odot$ material.

When no phase transition occurs, a maximum central density of 2.76 $n_{nuclear}$ is reached. Then the material rebounds. An equilibrium configuration is reached with a central density of 2.29 $n_{nuclear}$. When a phase transition occurs, the higher adiabatic index of the quark phase halts the collapse at a density slightly greater than the density where the phase transition ends. All baryons in approximately the first 15 or so zones of the simulation are in the pure quark phase. The core then rebounds to a lower density.

Table 2 lists the results of the collapses and summarizes the final state of the core at 104.5 ms, approximately 2.5 ms after bounce. It lists the maximum core mass density n_{max}, the final core density n_{equ}, the gravitational potential energy V, the internal energy T, and the differences ΔV and ΔT between collapses involving a phase transition and the collapse without one. $\Delta V < 0$ implies less energy in the shock; $\Delta V > 0$ implies more energy. The maximum shock kinetic energy is also listed. This is defined as the (Newtonian) kinetic energy mv^2 of all zones moving outward (i.e., zones having a positive velocity). M_{quark}, is the gravitational mass of material in the equilibrium core with a density greater than that at which the phase transition begins. That is, M_{quark} is the mass of all material which is wholly in the quark phase or is a mixture of quark phase and hadronic matter.

Table 2 shows that some of the phase transitions make more energy available to the shock, while others make less energy available. The determining factor is how compact the core becomes. Denser cores allow more gravitational potential energy to be released as internal and kinetic energy. The final density of the core depends on the width of the phase transition, since a wide phase transition allows more material to compress into a denser state.

Most of the phase transitions studied resulted in a core with quark matter in the center. Because the adiabatic index of the quark phase is so large, the final central density of the core is

TABLE 2

COMPARISON OF VARIOUS TRANSITIONS

Phase Transition	Order	n_{max}	n_{eq}	V	ΔV	T	ΔT	KE_{max}	M_{quark}
No transition		2.76	2.29	−54.79	...	59.94	...	0.0524	...
1.5 → 1.5	2	1.67	1.62	−51.74	−3.05	57.30	−2.64	0.0140	0.245
1.5 → 2.0	1	2.32	2.21	−56.91	+2.12	62.12	−2.18	0.0406	0.245
1.5 → 2.5	1	2.95	2.82	−62.18	+7.39	67.92	+7.98	0.0958	0.307
1.5 → 2.57	1	3.09	2.91	−63.00	+8.21	68.84	+8.90	0.103	0.315
2.0 → 2.0	2	2.17	2.07	−54.49	−0.30	59.62	−0.32	0.0243	0.0459
2.0 → 2.5	1	2.76	2.60	−56.47	+1.68	62.08	+2.14	0.0598	0.083
2.0 → 2.71	1	3.04	2.84	−57.58	+2.79	63.48	+3.54	0.0707	0.102
2.5 → 2.5	2	2.59	2.29[a]	−54.79	0.0	59.94	0.0	0.0500	...
2.5 → 2.87	1	2.94	2.29[a]	−54.79	0.0	59.94	0.0	0.0573	...

NOTES.—The maximum and equilibrium central densities, n_{max}, and n_{eq}, are given in units of nuclear density. V and T are the equilibrium potential and thermal energies, respectively, while KE_{max} is the maximum shock kinetic energy. The ΔV column shows how much more binding energy is released by the core as a result of the given phase transition. The ΔT column gives the difference in the thermal energy of the core. Positive entries in both columns indicate that more energy is released; negative numbers indicate that less energy is released. All energies are given in units of 10^{51} ergs. n_{eq}, V, T, and M_{quark} are measured at $t = 0.1045$ s, approximately 2 ms after bounce. M_{quark} is in $M_\odot$. T and V are integrals (eqs. [5] and [6], respectively) over the inner 0.5 $M_\odot$ of material.

[a] These cores settled back into nuclear matter.

only slightly greater than the quark phase equilibrium density. For the transitions beginning at 2.5 times nuclear matter density, the core entered the quark phase but bounced out of it. The core that finally resulted was composed entirely of hadronic matter.

In equilibrium, matter will tend not to be in a mixture of the two phases. The weight of matter farther from the center will compress the material in the less dense phase into the more dense phase. Very little matter will have a density between $n_{\rm hadron}$ and $n_{\rm quark}$. Because of this, a phase transition with a large coexistence region will allow more matter to enter the denser phase than a phase transition with a small coexistence region and the same final density. Thus, more energy was released by the phase transitions with $n_{\rm hadron} = 1.5$, $n_{\rm quark} = 2.0$ and $n_{\rm hadron} = 1.5$, $n_{\rm quark} = 2.5$ than by those with $n_{\rm hadron} = 2.0$, $n_{\rm quark} = 2.0$ and $n_{\rm hadron} = 2.0$, $n_{\rm quark} = 2.5$.

A core with a center of quark matter may have a central density less than the central density that occurs when no phase transition takes place. The average density of the core may be greater, however, because, more matter is in the denser phase. Thus, a core with a central density lower than the equilibrium density that occurs when there is no phase transition, may have $\Delta V \geq 0$. This is what occurred, for example, in the phase transition with $n_{\rm hadron} = 1.5$, $n_{\rm quark} = 2.0$ in Table 2.

The core collapses studied here fall into three classes. In the first, less energy is given to the shock when the quark phase equilibrium density is much less than the final density of the core in the model with no phase transition. The high adiabatic index of the quark phase causes the core to bounce and come to a final density which is not much greater than the equilibrium density of the quark phase. Because the final density of the core is smaller than when there is no phase transition, less gravitational binding energy is released. One example of this is the second-order phase transition with $n_{\rm hadron} = 1.5$, $n_{\rm quark} = 1.5$. The collapse halts at a lower density than when there is no phase transition, and the final density of the core is lower. Narrow phase transitions occurring at low density provide less energy to the shock. The core is less compact, and less binding energy is released. These transitions have $\Delta V < 0$ in Table 2.

The second class of phase transitions does not produce a significant difference in the binding energy of the core. There are two different processes that can produce this result. Some of these cases have quark cores, but coincidentally have gravitational potentials approximately equal to that of the core that results when no phase transition occurs. The phase transition with $n_{\rm hadron} = 2.0$, $n_{\rm quark} = 2.0$ is an example of this. The second process occurs for the phase transitions with $n_{\rm hadron} = 2.5$. The core does not remain in the quark phase. It rebounds to the same equilibrium density as when no phase transition occurs, and so the binding energy is the same. The proto-neutron stars left in these cases are not distinguishable from the remnant left when no phase transition occurs. However, an examination of the neutrino signal may provide a way to distinguish between collapses with and without a phase transition that does not leave behind a quark core.

In the third class of phase transitions in Table 2, a significant amount of binding energy is released. This happens because the equilibrium density of the core is greater than that reached when there is no phase transition. This occurs even though the collapse stops at a lower maximum density when a phase transition occurs. The equilibrium density is generally slightly greater than that of the quark phase; these collapses produce proto-neutron stars with quark cores, as well as making more internal energy available to power the shock. An example is the phase transition with $n_{\rm hadron} = 2.0$, $n_{\rm quark} = 2.71$. The final density of the core is greater, so more gravitational binding energy is released.

Our observed trend toward greater energy release in wider phase transitions differs from the results reported by Takahara & Sato (1985, 1986). They found that the energy released increased with the density at which the phase transition began. This result seems counterintuitive for two reasons. First, a larger coexistence region allows the core to become more dense, releasing more gravitational potential energy. Second, supernovae simulations have consistently yielded the result that softening the EOS above nuclear densities increases the shock strength. Our results are in agreement with this.

Figures 3 and 4 illustrate examples of the first and third class of phase transitions, specifically $n_{\rm hadron} = 1.5$, $n_{\rm quark} = 1.5$ and $n_{\rm hadron} = 2.0$, $n_{\rm quark} = 2.71$. We will refer to these as the shallow and deep phase transitions, respectively. These are compared to a collapse in which no phase transition takes place. Figure 3*a* shows the time evolution of the central density of the star. The stiffness of the quark phase stops the collapse at a central density slightly higher than $n_{\rm quark}$, and the equilibrium central density is approximately $n_{\rm quark}$. Figure 3*b* shows the shock kinetic energy, Figure 3*c* shows the shock velocity. The shock velocity was defined as the largest positive velocity of a zone in the simulation. The deep phase transition results in a higher maximum kinetic energy but not a higher maximum velocity than when no phase transition occurs. The shallow phase transition causes lower kinetic energy and velocity. The kinetic energy and velocity for both phase transitions converges to the value which results when there is no phase transition as the simulation proceeds. We expect that this would not be true if neutrinos were included in the simulation, because the amount of internal energy in the cores would be different. Figure 3*d* plots velocity as a function of radius at the time of maximum kinetic energy for the examples. The deep phase transition results in a higher velocity for a greater mass of matter than if no phase transition occurs. The shallow phase transition results in a smaller velocity and smaller mass of outward moving material.

Figure 4*a* displays density versus radius; Figure 4*b* displays energy density versus radius. The core in the deep phase transition case would have much more internal energy to power the shock through delayed mechanisms than when no phase transition occurs; the shallow phase transition would yield less internal energy.

Figures 5 and 6 show the two phase transitions in Table 1 with $n_{\rm hadron} = 2.5$, with the results from a collapse with no phase transition for comparison. The collapse stops at a density slightly higher than $n_{\rm quark}$, but the cores bounce out of the quark phase. Figure 5*a* shows that the central density rises above $n_{\rm quark}$, but quickly relaxes to the value it assumes when there is no phase transition. Figures 5*b* and 5*c* show that the shock kinetic energy and shock velocity are not very different when one of these phase transitions occurs, except very soon after bounce. Figures 6*a* and 6*b* compare the density and energy density of the cores with these phase transitions to the density and energy density of the core that results when there is no phase transition. The cores are virtually identical. In particular, there is no excess internal energy that might affect the delayed shock mechanism.

The shock in a supernova forms when the EOS stiffens and begins to halt the collapse. For the phase transitions we investigated, there are two changes in the EOS that can give rise to shocks. The EOS becomes much stiffer when nuclear density is reached, and also becomes much stiffer when the quark phase is entered. A core undergoing a phase transition could be expected to give rise to two shocks. The second shock, which is traveling through material that has already been heated, will travel faster and overtake the first shock, at which time the two shocks will coalesce. Figures 7 and 8 show this behavior for the EOS with $n_{\rm hadron} = 2.0$, $n_{\rm quark} = 2.71$.

Figure 7 plots density versus time for every third zone in the innermost $M_\odot$ of the simulation. Shocks show up as sudden changes in the density, i.e., nearly vertical lines on the graphs. Collapse and bounce with a phase transition is shown in Figure 7*a*; the corresponding behavior when no phase transition occurs is shown in Figure 7*b*. In both figures, it is clear that the innermost part of the core does not experience a shock; the shock forms farther out. Two distinct shocks can be seen in Figure 7*a*. The first propagates outward from the central zones as the density surpasses nuclear matter density. This shock forms at about $t = 0.1018$. Another shock develops as the inner zones enter the quark phase. This shock forms at about $t = 0.1020$, and coalesces with the first shock at about $t = 0.1021$. There is only one shock in Figure 7*b*, which shows the evolution of a core in which no phase transition took place. This second shock has also been seen by Takahara & Sato (1985, 1986).

The evolution of velocity and density with time is shown for six Lagrangean sections of the simulation in Figures 8*a* through 8*f*. These sections have interior masses of 0.096, 0.245, 0.366, 0.459, 0.552, and 0.638 $M_\odot$, respectively. These are the

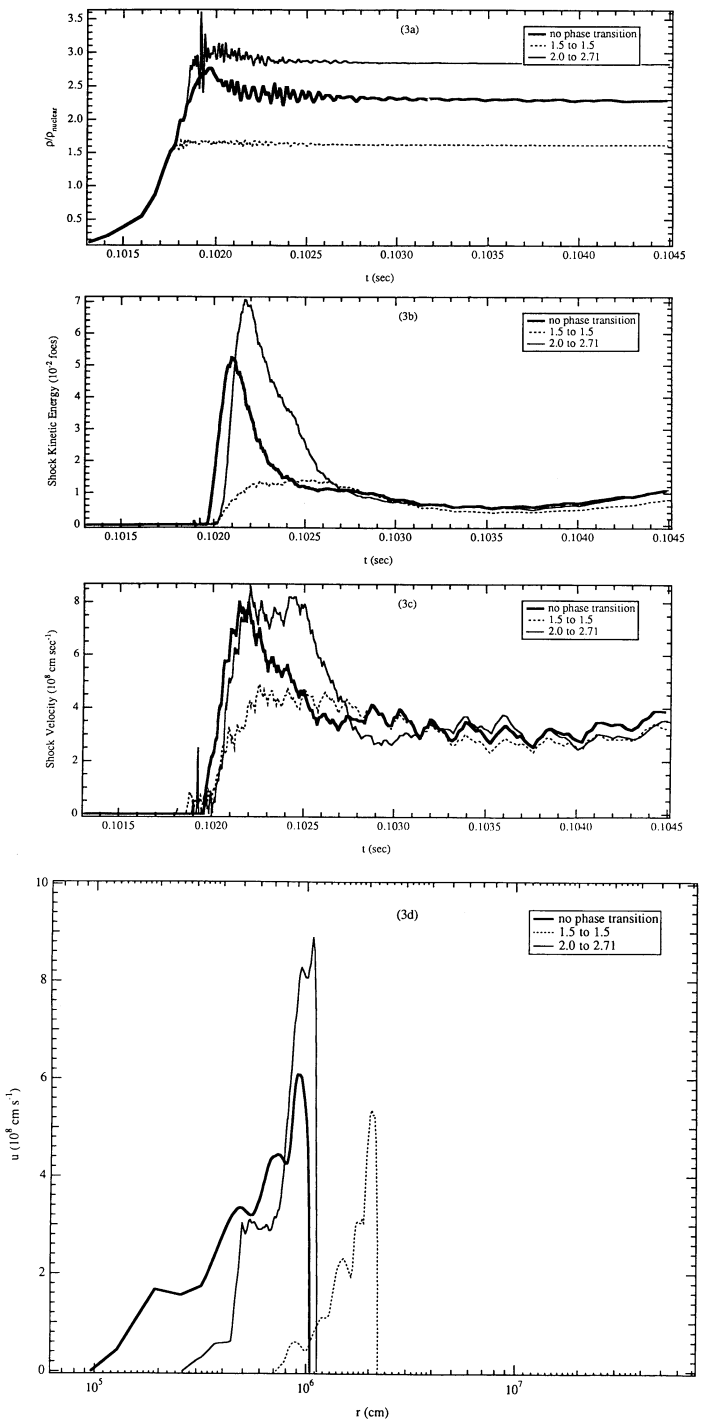

FIG. 3.—Time development of cores udergoing phase transitions compared to a core with no phase transition (*heavy line*). (*a*) Central density ρ as a function of time t. (*b*) Shock kinetic energy vs. t. (*c*) Shock velocity u vs. t. (*d*) Velocity u vs. radius r at the time of maximum shock kinetic energy. The velocity for the EOS with no phase transition is plotted at $t = 0.102103$; for the deep phase transition at $t = 0.102169$; for the shallow phase transition at $t = 0.102540$.

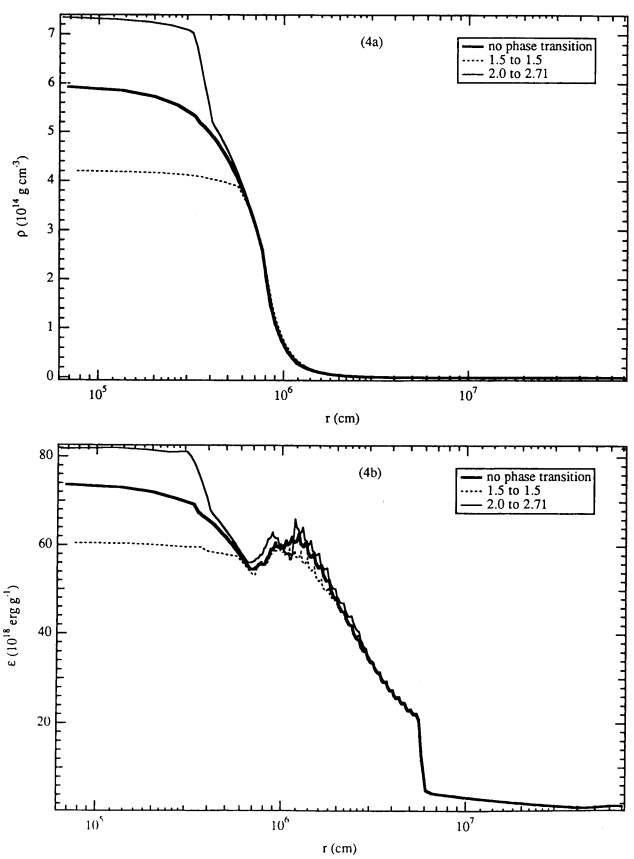

FIG. 4.—Configuration of cores at $t = 0.1045$ seconds after collapse begins. (*a*) Density ρ as a function of radius r. (*b*) Energy density ϵ vs. r.

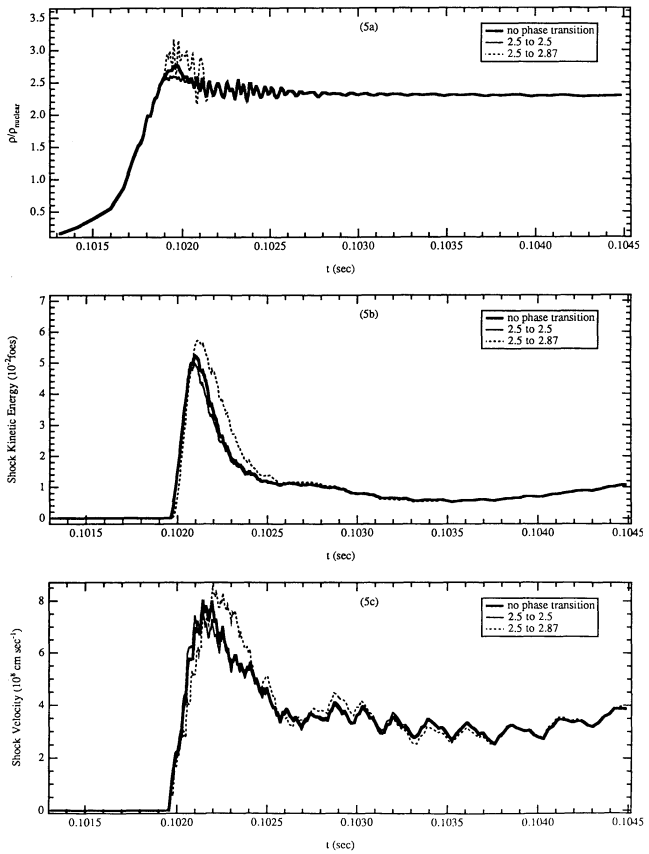

FIG. 5.—Time development of cores which undergo phase transitions but in which no matter remains in the quark phase, compared to a core with no phase transition (*heavy line*). (*a*) Central density ρ as a function of time t. (*b*) Shock kinetic energy vs. t. (*c*) Shock velocity u vs. t.

5th, 10th, 15th, 20th, 25th, and 30th zones of Figure 7*a*. The behavior of the second shock can be seen in these graphs as a sudden increase in density coupled with a sudden decrease in the magnitude of the velocity (which is negative during the collapse). Figure 8*a* shows the first shock occurring slightly before $t = 0.1018$. The speed of infall increases again when pressure support from interior zones is removed as they enter the phase transition. The second shock follows soon after; density increases sharply and the magnitude of the velocity decreases sharply. The changes associated with both shocks are of approximately equal magnitude for this epoch.

In Figures 8*b* through 8*e*, the size of the changes associated with the second shock becomes smaller relative to the changes associated with the first shock. The second shock also follows the first one more closely in time. The quantities in Figure 8*f* show only one sharp change. The shocks have coalesced into one shock by the time this section is shocked, at $t = 0.1021$.

Calculating the evolution beyond this point requires more detailed modeling of the matter equation of state and inclusion of neutrino transport mechanisms. Work along these lines is currently in progress.

6. CONCLUSIONS

We have used a spherically symmetric general relativistic hydrodynamics code to investigate the effects of the QCD phase transition on supernovae core collapse. The temporal development of the central core density was studied using the BCK nuclear equation of state to describe hadronic matter and a QCD-motivated equation of state for the quark-gluon plasma. Collapsing stellar cores that evolved through phase transitions were compared to the core that developed when there was no phase transition. Differences in the gravitational binding energy and internal energy of these models were calculated. The amount of extra gravitational potential energy yielded from collapses with a phase transition with a large coexistence region was significant, on the order of 10^{52} ergs, whereas phase transitions with small phase coexistence regions were observed to yield less energy to the shock. The largest amount of internal energy in the core made available by phase transitions was also on the order of 10^{52} ergs. Examination of the density and velocity profiles during a collapse with a phase transition shows that soon after bounce there are two shocks. One is caused by the stiffening of the equation of state when nuclear density is reached, the other by the stiffening of the EOS when the quark phase is reached. The second shock, proceeding through matter heated by the first shock, overtakes and coalesces with the first approximately one-tenth of a millisecond after it forms.

Our study provides us with an understanding of some of the effects of phase transitions on core dynamics that will aid us in subsequent calculations of the long-term development of the core, and the emitted neutrino signals. An effect which we have not modeled here is an additional neutrino burst that may occur when the quark phase is produced. The conversion of up

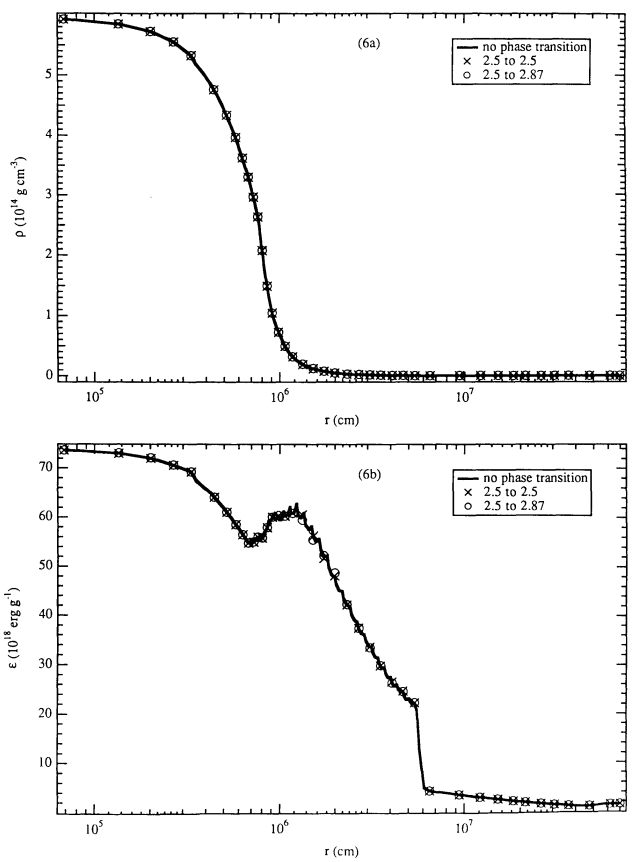

FIG. 6.—Configuration of cores which undergo phase transitions but in which no matter remains in the quark phase. Time is 0.1045 seconds after collapse begins. (*a*) Density ρ as a function of radius r. (*b*) Energy density ϵ vs. r.

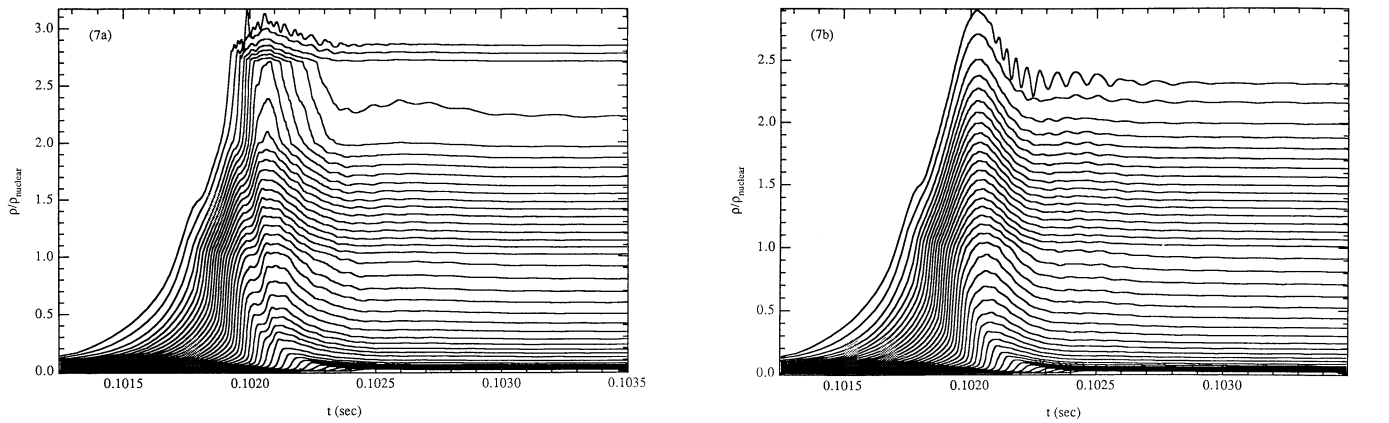

FIG. 7.—Density ρ vs. time t for Lagrangean sections of the core. Shocks show as sudden changes in density, where the lines become nearly vertical. (*a*) Core in which a phase transition from 2.0 to 2.71 times nuclear density took place. For a time, two separate shocks can be seen (*b*). Core in which no phase transition occurred.

and down quarks to strange quarks is a weak interaction that will emit neutrinos. There are also other possible phase transitions, e.g., pion or kaon condensates. These effects will be studied in subsequent work. Our results may be important in determining whether or not a black hole forms, and this in turn may be important in determining whether or not there is a viable supernova explosion.

The authors acknowledge useful discussions with N. J. Snyderman, J. L. Hughes, J. R. Wilson, R. W. Mayle, D. S. Miller, G. E. Brown, J. Cooperstein, and J. M. Lattimer. N. A. G. thanks the Fannie and John Hertz Foundation for a fellowship which partially supported this work. F. D. S. wishes to acknowledge financial support under US Department of Energy grant no. DE-FG02-87ER40317, and supercomputing

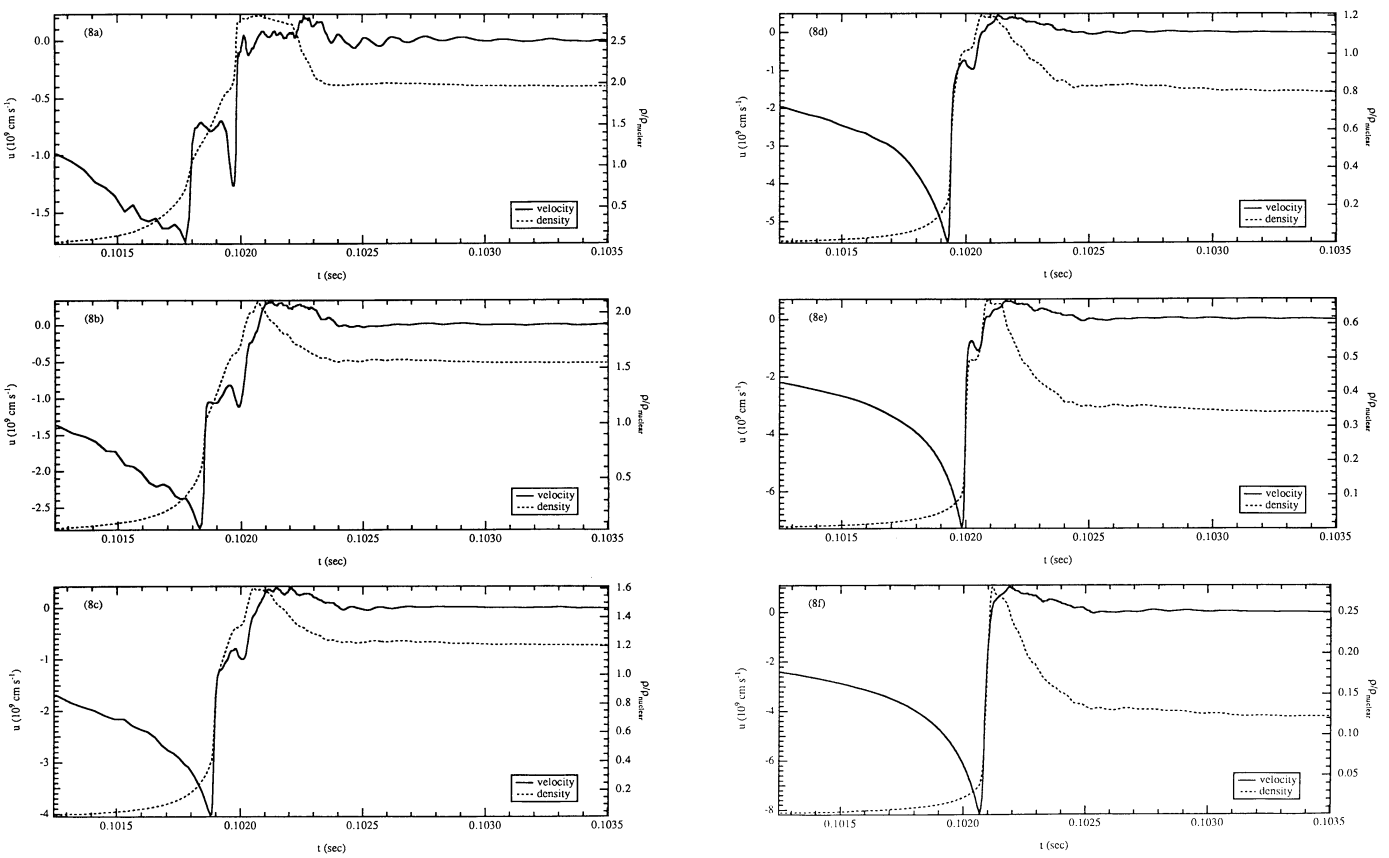

FIG. 8.—Density ρ and velocity u vs. time t for several Lagrangean sections of a collapsing core undergoing a phase transition from 2.0 to 2.71 times nuclear density Sudden changes corresponding to shocks show as vertical lines. Two shocks can be seen, which approach one another and finally coalesce. (*a*) 0.096 $M_\odot$, (*b*) 0.245 $M_\odot$, (*c*) 0.366 $M_\odot$, (*d*) 0.459 $M_\odot$, (*e*) 0.552 $M_\odot$, (*a*) 0.638 $M_\odot$.

support from the Pittsburgh and NERSC supercomputing centers. Work at Lawrence Livermore National Laboratory was performed under the auspices of the US Department of Energy under contract no. W-7405-ENG-48 and DOE Nuclear Theory grant SF-ENG-48. This work was also partially supported at UCSD by NSF grant PHY 91-21623 and IGPP grant 93-22.

REFERENCES

Alcock, C., Farhi, E., & Olinto, A. 1986, ApJ, 310, 261
Alcock, C., Fuller, G. M., & Mathews, G. J. 1987, ApJ, 320, 439
Baron, E. A., Cooperstein, J., & Kahana, S. 1985a, Phys. Rev. Lett., 55, 126
———. 1985b, Nucl. Phys. A, 440, 744
Baron, E. A. 1985, Ph.D. thesis, State Univ. New York, Stony Brook
Baym, G., & Chin, S. A. 1976, Phys. Lett., 62B, 241
Berg, B., et al. 1986, Z. Phys. C, 31, 167
Bethe, H. A., Brown, G. E., & Cooperstein, J. 1987, Nucl. Phys. A, 462, 791
Bethe, H. A., et al. 1979, Nucl. Phys. A, 324, 487
———. 1983, Nucl. Phys. A, 403, 625
Bethe, H. A., & Wilson, J. R. 1985, ApJ, 295, 14
Bowers, R. L., & Wilson, J. R. 1982, ApJS, 50, 115
Brown, F. R., et al. 1988, Phys. Rev. Lett., 61, 2058
———. 1990, Phys. Rev. Lett., 65, 2491
Bruenn, S. W. 1989a, ApJ, 340, 955
———. 1989b, ApJ, 341, 385
Bruenn, S. W., Arnett, W. D., & Schramm, D. N. 1977, ApJ, 213, 213
Burrows, A., & Fryxell, B. 1992, Science, 258, 430
Callen, C. G., Dashen, R. F., & Gross, D. J. 1979, Phys. Rev. D, 19, 1826
Chandrasekhar, S. 1969, Hydrodynamic and Hydromagnetic Stability (New York: Dover)
Colgate, S. A., & White, R. H. 1966, ApJ, 143, 626
Collins, J. C., & Perry, M. J. 1975, Phys. Rev. Lett., 34, 1353
Cooperstein, J., & Baron, E. A. 1990 in Supernovae, ed. A. Petschek (New York: Springer), 213
Cooperstein, J., Bethe, H. A., & Brown, G. E. 1985, Nucl. Phys. A, 429, 527
Farhi, E., & Jaffe, R. L. 1984, Phys. Rev. D, 30, 2379
Freeman, B. A., & McLerran, L. D. 1977a, Phys. Rev. D, 16, 1130
———. 1977b, Phys. Rev. D, 16, 1147
———. 1977c, Phys. Rev. D, 16, 1169
Friedman, B., & Pandharipande, V. R. 1981, Nucl. Phys. A, 361, 502
Fuller, G. M., Mathews, G. J., & Alcock, C. R. 1988, Phys. Rev. D, 37, 1380
Harrison, B. K., et al. 1965, Gravitation Theory and Gravitational Collapse (Chicago: Univ. Chicago Press)
Herant, M., Benz, W., & Colgate, S. 1992, ApJ, 395, 642
Landau, L. D., & Lifshitz, E. M. 1980, Statistical Physics (3d ed.; Oxford: Pergamon Press)
Lattimer, J. M., & Swesty, F. D. 1991, Nucl. Phys. A, 535, 331
Livio, M., Buchler, R. J., & Colgate, S. A. 1980, ApJ, 238, L139
May, M., & White, R. 1967, in Methods of Computational Physics, Vol. 7, ed. B. Alder, S. Fernbach, & M. Rotenberg (New York: Academic Press), 219
Mayle, R. W. 1990, in Supernovae, ed. A. Petschek (New York: Springer), 267
Mazurek, T. J. 1975, Ap&SS, 35, 117
McLerran, L. 1986, Rev. Mod. Phys., 58, 1021
Miller, D. S., Wilson, J. R., & Mayle, R. W. 1992, preprint
Myra, E. S., & Bludman, S. A. 1989, ApJ, 340, 384
Nomoto, K., & Hashimoto, M. 1988, Phys. Rep., 163, 13
Pethick, C. J., Ravenhall, D. G., & Lattimer, J. M. 1984, Nucl. Phys. A, 414, 517
Polyakov, A. M. 1978, Phys. Lett., 72B, 477
Schramm, D. N., & Arnett, W. D. 1975, ApJ, 198, 629
Shapiro, S. L., & Teukolsky, S. A. 1983, Black Holes, White Dwarfs, and Neutron Stars (New York: Wiley)
Smarr, L., et al. 1981, ApJ, 246, 515
Susskind, L. 1979, Phys. Rev. D, 20, 2610
Takahara, M., & Sato, K. 1985, Phys. Lett., 156B, 17
———. 1986, Ap&SS, 119, 45
Van Riper, K. A. 1979, ApJ, 232, 558
Van Riper, K. A., & Arnett, W. D. 1978, ApJ, 225, L129
Walhout, T. S. 1988, Nucl. Phys. A, 484, 397
———. 1990, Nucl. Phys. A, 519, 816
Wambach, J. 1990, Lectures given at the Spring School on Medium- and High-Energy Nuclear Physics (Tainan, Republic of China)
Weinberg, S. 1972, Gravitation and Cosmology: Principles and Applications of the General Theory of Relativity (New York: Wiley)
Wilson, J. R. 1985, in Numerical Astrophysics, ed. J. M. Centrella, J. M. LeBlanc, & R. L. Bowers (Boston: Jones and Bartlett), 422
Wilson, J. R., & Mayle, R. W. 1988, Phys. Rep., 163, 63
Witten, E. 1983, Nucl. Phys. B, 223, 422
———. 1984, Phys. Rev. D, 30, 272

Note added in proof.—It has recently come to our attention that a similar study has been made by J. Cooperstein (*Nucl. Phys.*, in press). He finds similar results with regard to the coexistence region increasing the energy of the shock but does not see a secondary shock from the phase transition. Cooperstein concludes that the electron equation of state mutes the transition. However, our study also included electrons in the equation of state and did see secondary shocks. The source of this difference is not clear at present.